Journal of South American Earth Sciences xxx (xxxx) 105170

Contents lists available at ScienceDirect

Journal of South American Earth Sciences

journal homepage: www.elsevier.com/locate/jsames

Basement reactivation and structural inheritance in the Jurassic to Neogene evolution of the North Patagonian Andes (41° 08' – 41° 11' S), Argentina

Sofía Peltzer [a,*], María Belén Yoya [a], Ezequiel Olaizola [b], Florencia Bechis [b], Daniel Yagupsky [c], Pablo D. González [d], Miguel A. S. Basei [e], Sebastián Oriolo [a]

[a] CONICET-Universidad de Buenos Aires, Instituto de Geociencias Básicas, Aplicadas y Ambientales de Buenos Aires (IGEBA), Intendente Güiraldes 2160, C1428EHA, Buenos Aires, Argentina
[b] CONICET-Universidad Nacional de Río Negro, Instituto de Investigaciones en Diversidad Cultural y Procesos de Cambio, Bartolomé Mitre 630, R8400AHN, San Carlos de Bariloche, Argentina
[c] CONICET- Universidad de Buenos Aires, Instituto de Estudios Andinos (IDEAN), Intendente Güiraldes 2160, C1428EHA, Buenos Aires, Argentina
[d] CONICET-SEGEMAR, Regional Sur, Independencia, 1495, Parque Industrial 1, R8332EXZ, General Roca, Argentina
[e] Universidade de São Paulo, Centro de Pesquisas Geocronologicas, Instituto de Geociências, Rua do Lago 562, CEP 05508-080, São Paulo, Brazil

ARTICLE INFO

Keywords:
Patagonian basement
North Patagonian batholith
Jurassic transtension
Neogene transpression

ABSTRACT

Structural inheritance is a major control on the Andean structural architecture and magma emplacement, particularly in Patagonia, where the genesis of sedimentary basins and magmatic arcs has been largely influenced by basement fabrics. Based on new geologic, structural, microstructural and geochronologic data, the aim of this contribution is to evaluate the influence of pre-existing mechanical anisotropies of the Paleozoic basement on the Jurassic-Neogene tectonic evolution in the Paso de las Nubes area (North Patagonian Andes, Argentina). U-Pb zircon data of an orthogneiss yielded an age of 166 ± 2 Ma, which is consistent with the Jurassic batholith reported in the North Patagonian Andes, being thus coeval with retrograde metamorphism and deformation in the metasedimentary wallrock. Fault kinematic data indicate a Jurassic transtensional regime, strongly controlled by basement reactivation. On the other hand, a second kinematic population records a mainly strike-slip solution, associated with partitioned Neogene transpression.

1. Introduction

Crustal deformation commonly tends to locate preferentially in pre-existing mechanical weaknesses, such as pre-existing shear zones and rheological heterogeneities, instead of generating new structures (White et al., 1986; Clendenin and Diehl, 1999; Thatcher, 1995; Holdsworth et al., 2001a, 2001b; Butler et al., 2006; Şengör et al., 2018; Schiffer et al., 2020). Thus, structural inheritance refers to the influence exerted by pre-existing structures in subsequent deformation processes, which imply rejuvenation (Salazar-Mora et al., 2018; Schiffer et al., 2020). The latter may involve either reactivation or reworking, depending on whether deformation localization occurs in heterogeneities formed during earlier tectonic events or the recurrent location of magmatism, metamorphism and other thermal processes is observed in the same lithospheric areas, respectively (Sutton and Watson, 1986; Holdsworth et al., 1997, 2001a, 2001b). Rejuvenation is commonly promoted by crustal weakening due to coupled processes that take place in shear zones, such as strain softening, and melt and hydrothermal fluid circulation (Davidson et al., 1994; Holdsworth et al., 1997).

In the Patagonian region, inherited basement structures, such as regional metamorphic and mylonitic fabrics related to Paleozoic medium- to high-grade metamorphism and deformation, commonly control the Mesozoic to Cenozoic development of volcano-sedimentary basins, hydrothermal ore deposits and magmatic bodies (e.g., Renda et al., 2019, and references therein; Giacosa, 2020; Benedini et al., 2021; García et al., 2024). The existence of Paleozoic basement mechanical anisotropies has thus been proposed to explain the localization of intraplate deformation during different tectonic events (Bilmes et al., 2013; Echaurren et al., 2016; Gianni et al., 2015, 2017; Renda et al., 2019; García et al., 2024). In particular, the role of the basement is critical in the Andean evolution of the North Patagonian Andes, which comprises a thick-skinned fold and thrust belt with an eastward vergence (Giacosa and Heredia, 2004a, 2004b; Giacosa et al., 2005; Bechis and Cristallini, 2006; Ramos et al., 2014; Orts et al., 2015).

* Corresponding author.
E-mail address: sofiapeltzer@gmail.com (S. Peltzer).

https://doi.org/10.1016/j.jsames.2024.105170
Received 7 June 2024; Received in revised form 10 August 2024; Accepted 18 September 2024
0895-9811/

The present work is focused on basement rocks of the Paso de las Nubes area, which is located to the west of the city of San Carlos de Bariloche, Río Negro province, Argentina (Fig. 1). This area is part of the Andean thick-skinned fold and thrust belt of the North Patagonian Andes. Since there is a widespread Jurassic magmatism recorded in this sector, likely associated with retrograde metamorphism and deformation of basement fabrics, new geologic, structural, kinematic, microstructural and geochronologic data are provided, in order to evaluate the role of basement fabrics during the Jurassic to Neogene construction of the region.

2. Geologic setting

2.1. Regional geologic framework

The North Patagonian Andes (NPA) are located in the southernmost region of the Central Andes and north of the Chilean Triple Junction, between the Chilean Central Valley to the west and the North Patagonian Massif to the east (Fig. 1; Giacosa and Heredia, 2004a, 2004b; Giacosa et al., 2005; Oriolo et al., 2019). The basement of the northern sector of the NPA is mainly represented by the Bariloche Complex (Oriolo et al., 2019), which records Devonian to Carboniferous high- to medium-grade metamorphism and a main WNW-ESE to NNW-SSE-trending foliation (García-Sansegundo et al., 2009; Martínez et al., 2012, 2023; Oriolo et al., 2019) and was intruded by the Carboniferous Guillelmo-Serrucho Plutonic Complex, recently defined by Yoya et al. (2023).

The region was covered by volcano-sedimentary successions of the Cordilleran Volcano-Sedimentary Complex during the Jurassic (Giacosa and Heredia, 2000; Giacosa et al., 2001). Furthermore, multiple pulses of Mesozoic to Cenozoic arc magmatism are also documented. The Cordilleran Patagonian Batholith constitutes a prominent characteristic of the North Patagonian Andes and represents the magmatic arc associated with subduction along the Paleo-Pacific margin (Giacosa et al., 2001). This batholith is mainly composed of calc-alkaline intrusive intermediate to acidic rocks, comprising tonalities, Qz-diorites, monzogranites, granodiorites and granites of Jurassic to Miocene ages (Toubes and Spikerman, 1973; González Díaz, 1982; Rapela et al., 1987; Castro et al., 2011; Aragón et al., 2011; Hervé et al., 2018; Zaffarana et al., 2020; Boltshauser et al., 2023), although Cretaceous intrusions are also recorded further north (Gregori et al., 2011). There is also a previous Jurassic calc-alkaline magmatic pulse recorded in the NPA, which is constrained to the Early Jurassic NNW-SSE striking Subcordilleran Patagonian Batholith (Gordon and Ort, 1993; Haller et al., 1999; Rapela et al., 2005; Zaffarana et al., 2020, 2024).

During the Jurassic, the northern Patagonian region was affected by widespread extensional/transtensional deformation (Giacosa and Heredia, 2004b; Castro et al., 2011; Orts et al., 2012; Tobal et al., 2012; Oriolo et al., 2019). In the NPA, this transtensional event was strongly influenced by reactivation of WNW-ESE- to NNW-SSE-striking basement fabrics that controlled the emplacement of Jurassic plutons (Castro et al., 2011; Oriolo et al., 2019). In addition, deposition of coeval volcano-sedimentary sequences was associated with N-S- to NNW-SSE-striking half-grabens, partly inverted by subsequent Andean deformation (Giacosa and Heredia, 2004a, 2004b). The onset of Andean compressional deformation occurred in the Cretaceous, giving rise to orogen-parallel thrusts (Orts et al., 2012; Tobal et al., 2012; Ramos et al., 2014; Echaurren et al., 2016, 2017; Gianni et al., 2018; Butler et al., 2020). After Cretaceous compression, the region underwent an Oligocene to Early Miocene extensional phase, associated with N-S- to

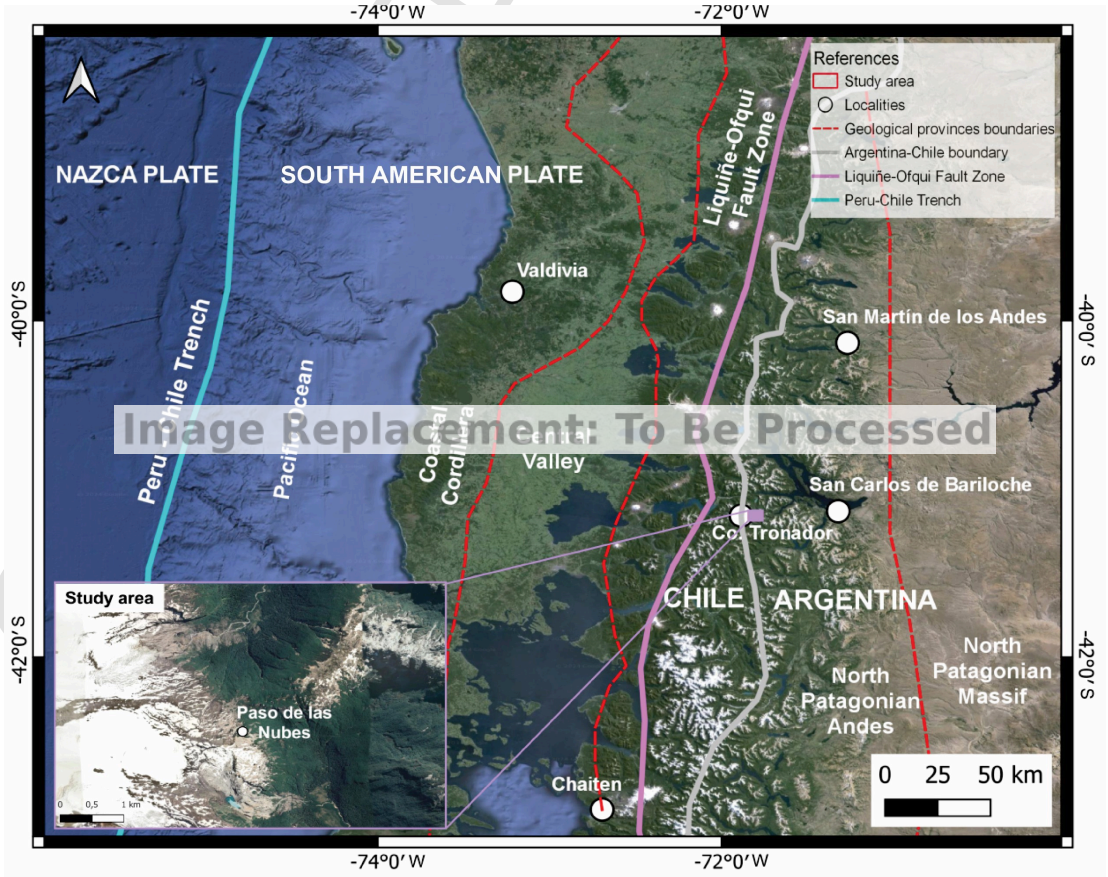

Fig. 1. Regional and tectonic sketch map showing the study area location (modified from Orts et al., 2015; Oriolo et al., 2019).

NW-SE-striking hemi-grabens (Orts et al., 2012; Tobal et al., 2012, 2015; Bechis et al., 2014; Ramos et al., 2014; Echaurren et al., 2016), which was followed by the Middle to Late Miocene Andean transpression (García et al., 2024).

Miocene Andean shortening promoted the development of a fold-and-thrust belt in the NPA, comprising NW-SE- to N-S-striking thrusts and back-thrusts (Giacosa and Heredia, 2004a, 2004b; Orts et al., 2012; Tobal et al., 2012; Bechis et al., 2014; Ramos et al., 2014, 2015; Echaurren et al., 2016). An internal, western zone is characterized by a thick-skinned fold and thrust belt, whereas the external or eastern zone is dominated by folding and thrusting of the deposits in the foreland Ñirihuau basin (Giacosa et al., 2005; Bechis and Cristallini, 2006). Additionally, Giacosa and Heredia (2004a, b) described thrusts and back-thrusts originated by tectonic inversion of an extensional Mesozoic system. On the other hand, kinematic data of minor NE-SW to NNE-SSW faults suggested that the North Patagonian Andes between 40° and 42° S were formed by a transpressional deformation regime during the Neogene (Diraison et al., 1998; García et al., 2024). Furthermore, the NPA structural architecture was also conspicuously influenced by the Liquiñe-Ofqui Fault Zone (LOFZ), which constitutes a N-S- to NNE-SSW-striking dextral transpressional fault system, over 1000 km long, that accommodates strike-slip deformation due to the oblique convergence between the Nazca and South American plates (Hervé et al., 1974; Hervé, 1976; Cembrano et al., 1996; Lavenu and Cembrano, 1999; Rosenau et al., 2006; Orts et al., 2015).

2.2. Local geology

The basement of the study area comprises schists and paragneisses, with subordinate amphibolites, orthogneisses and foliated granitoids (Fig. 2; Olaizola, 2017; Oriolo et al., 2019). It exhibits a N-S- to NNW-SSE-trending metamorphic foliation, with steep dips (Fig. 2). These rocks are overlain by the Early to Middle Jurassic Cordilleran Volcano-Sedimentary Complex, which includes andesitic to rhyodacitic volcanic and pyroclastic rocks, pelites, sandstones and conglomerates, though it is mainly represented by andesites in the Paso de las Nubes area (Giacosa et al., 2001; Olaizola, 2017).

On the other hand, Miocene granitic and granodioritic bodies of the Coluco Formation intrude both the Bariloche Complex and the Cordilleran Volcano-Sedimentary Complex (González Díaz, 1978). To the west, all successions are covered by the Pliocene-Pleistocene Tronador Volcanic Complex, comprising basaltic to andesitic lavas, pyroclastic and gravitational flow deposits and lahars, and hyaloclastic breccias (Mella et al., 2005; Olaizola, 2017). Finally, Holocene glacial, colluvial and alluvial deposits are recorded in the area (Villalba et al., 1990; Olaizola, 2017).

3. Materials and methods

One sample of orthogneiss (BA 21-18), intercalated with metasedimentary basement rocks of the North Patagonian Andes, was collected at the Paso de las Nubes area (Figs. 2 and 3B; 41°09′16.00″S, 71°47′40.60″W). Zircon U-Pb LA-ICP-MS geochronological analysis was carried out at the Geochronologic Research Center of the University of São Paulo (Brazil) using a Thermo Fisher Scientific Neptune multicollector inductively coupled plasma – mass spectrometer (ICP-MS). Analytical protocols and results are included in Supplementary Data 1. Geochronologic data were integrated with structural and microstructural evidence from the studied unit and its wallrock.

The structural analysis included measurement of the orientation of the basement metamorphic foliation, and faults affecting it. Different types of kinematic indicators in ca. 30 outcrop-scale faults were measured (Supplementary Data 2). These include slickensides (Fig. 3A), crystal fibers on slip planes, and associated, mainly Riedel fractures, following the criteria proposed by Petit (1987). The principal incremental shortening (P) and extension (T) axes were obtained for each fault (Marrett and Allmendinger, 1990). A visual inspection was carried out to select fault-slip data that are kinematically compatible, separating the dataset in compatible subsets. For each data subset, the principal axes of the strain ellipsoid have been computed using the moment tensor summation method as implemented in FaultKin® (Allmendinger, 2001).

4. Results

4.1. Field and microstructural characterization

4.1.1. Orthogneiss

Sample BA 21-18 corresponds to an orthogneiss, which comprises a leucocratic foliated body of ca. 32 cm thick, which lies parallel to the

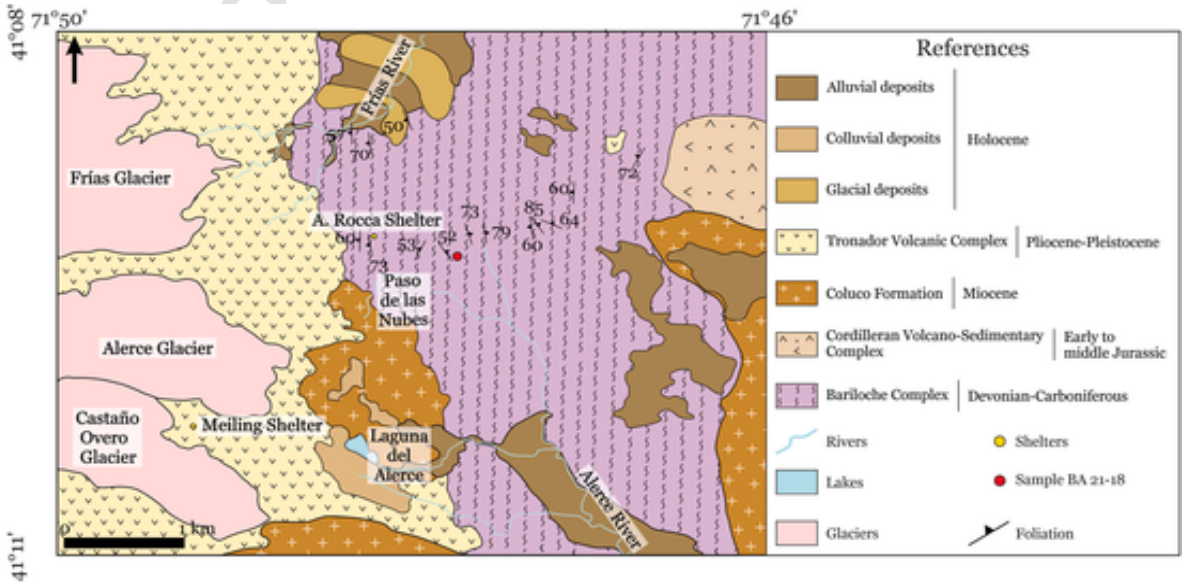

Fig. 2. Geologic map of the study area (modified from Olaizola, 2017).

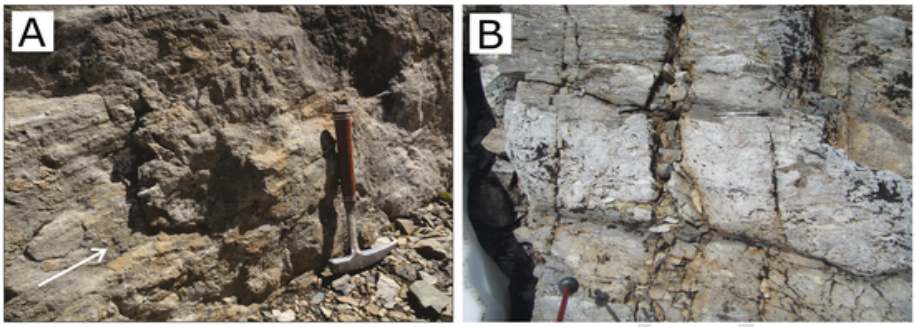

Fig. 3. A. Example of slickensides in mesoscale fault of the study area. The white arrow indicates the direction and sense of movement of the missing fault block. B. Felsic orthogneiss intercalation in basement metasedimentary rocks.

metamorphic foliation of the wallrock (Fig. 3B). However, a primary porphyritic texture is still slightly preserved in the rock under the microscope, showing approximately plagioclase euhedral porphyroclasts (10 %), probably corresponding to former phenocrysts. Porphyroclasts are surrounded by a foliated matrix (90 %), which is mainly composed of plagioclase (20 %), quartz (40 %), K-feldspar (35 %) and opaque minerals (5 %) (Fig. 4A). Plagioclase porphyroclasts, with an average size of 2 mm, are fractured and contain sericite, epidote and chlorite replacements. Relic quartz grains with undulose extinction and subgrains are observed, together with very fine-grained (< 10 μm) quartz aggregates with irregular boundaries. The latter are interpreted as products of dynamic recrystallization due to bulging and subordinate subgrain rotation (Fig. 4C).

A striking feature of the sample is the presence of radial fibrous intergrowths of quartz and K-feldspar, that seem to be locally circumscribed to ovoid bodies (Fig. 4B). They may correspond to deformed spherulites, though these intergrowths randomly occur in the matrix as well, showing a plumose aspect and not limited to discrete ovoid bodies. Another notable feature is the presence of granophyric intergrowths of quartz and K-feldspar, in some cases associated with strain shadows (Fig. 4D).

4.1.2. Metasedimentary wallrock

The wallrock corresponds to schists with a locally porphyroblastic microstructure. When present, plagioclase porphyroblasts of 0.8–1.2 mm occur within a preferred-oriented matrix composed of granoblastic quartz and lepidoblastic phyllosilicates between 200 and 600 μm grain size (Fig. 5A). The mineral assemblage comprises quartz, plagioclase, muscovite and chlorite. Accessory minerals such as tourmaline, zircon and rutile were also identified. There is also a moderate

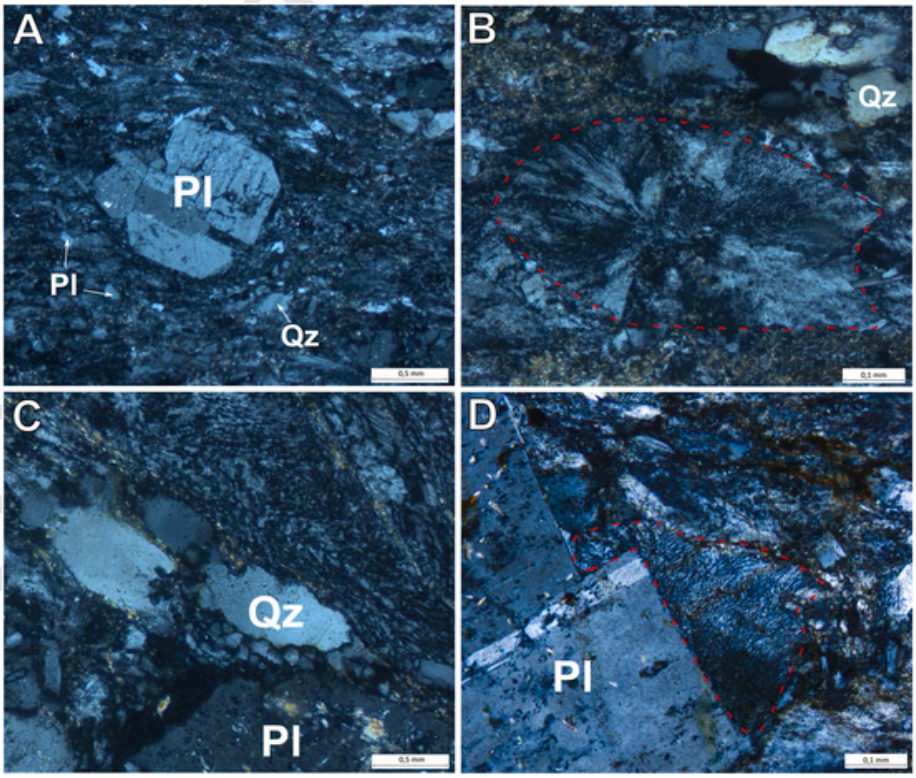

Fig. 4. Photomicrographs of the orthogneiss (crossed polars). A. Detail of matrix deflection around plagioclase (Pl) porphyroclast. B. Flattened spherulite (red dotted line). C. Bulging recrystallization around relic quartz (Qz) grains. D. Quartz and feldspar granophyric intergrowth (red dotted line) associated with porphyroclast strain shadows.

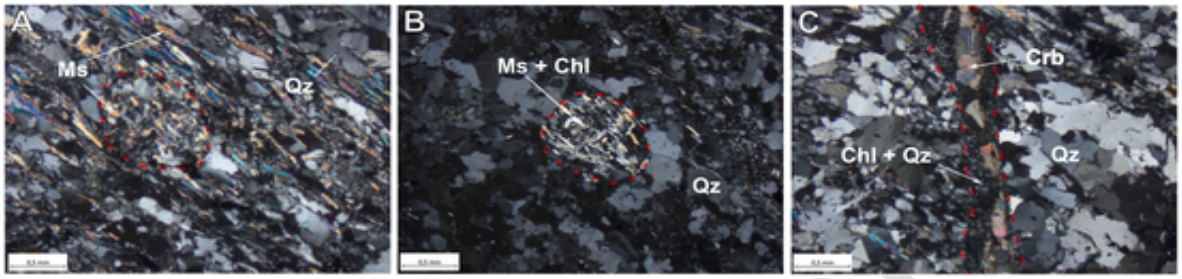

Fig. 5. Photomicrographs of schists of the Bariloche Complex (crossed polars). A. Metamorphic foliation composed of lepidoblastic muscovite (Ms) and granoblastic quartz (Qz), and replaced plagioclase porphyroblast (red dotted line). B. Retrograde fine-grained chlorite (Chl) and white mica replacing a plagioclase porphyroblast (red dotted line) and the matrix. C. Veinlet filled with chlorite-quartz microgranular aggregate and carbonates (Crb).

to pervasive retrograde overprint of randomly oriented fine-grained chlorite and white mica, both ranging from 50 to 200 μm grain size, cross-cutting the foliation and partly replacing plagioclase porphyroblasts (Fig. 5B). Additionally, discordant veinlets cross-cut the foliation, and are filled with carbonates and/or fine-grained quartz and chlorite (Fig. 5C).

4.2. U-Pb zircon geochronology

Zircons of sample BA 21-18 are euhedral to subhedral prisms, being mainly characterized by oscillatory zoning documented by cathodoluminescence images, thus indicating a magmatic origin. A concordia age of 166 ± 2 Ma (MSWD = 0.045, probability = 0.83) was obtained considering 17 out of 24 spots (Fig. 6; Supplementary Data 1). Following standard procedures, data were excluded for age calculation due to inheritance, high common Pb content and/or analytical problems. The obtained age is interpreted as the crystallization age of the magmatic protolith.

4.3. Structural and kinematic data

A total of 32 kinematic data from meso-scale faults were measured in the metamorphic wallrock. These structures mostly exhibit steep dips and, although their trends show some dispersion, a main N-S to NNW-SSE orientation and a secondary NNE-SSW orientation can be observed, which are parallel to the main trend of the metamorphic foliation (Fig. 7A and B). For the total population of faults, the obtained principal incremental shortening (P) and extension (T) axes display a significant dispersion, suggesting that they represent different populations. Therefore, data cannot be used to calculate a strain ellipsoid for the entire data set. A visual criterion was used to select kinematically compatible fault-slip data, and two groups of subsets were separated. The first subset is compatible with a transtensional strain regime, with an E-W extension direction and N-S oblique shortening (Fig. 7C). It comprises ENE-WSW left-lateral strike-slip faults, and NNW-SSE to NNE-SSW normal-oblique faults. Alternatively, the second subset shows a pure strike-slip solution, with a N-S extension direction and E-W shortening (Fig. 7D). NNE-SSW to NE-SW right-lateral strike-slip faults and NNW-SSE to

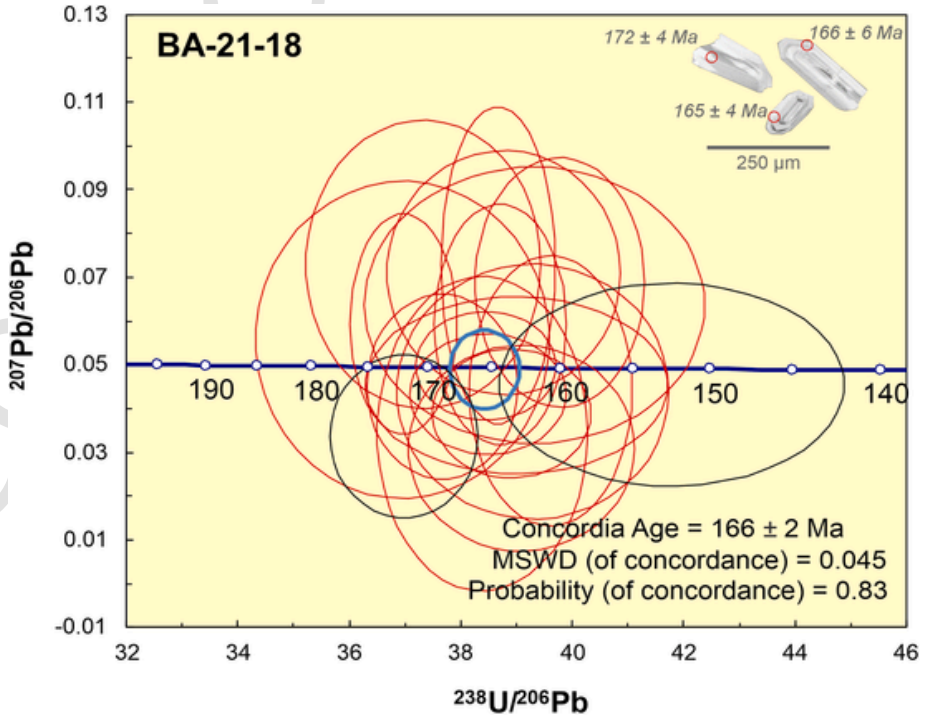

Fig. 6. U-Pb zircon age of the orthogneiss sample (BA 21-18). Concordia age (blue ellipse), data used for calculation (red ellipses) and discarded data (black ellipses) are indicated. All errors at 2σ level. Cathodoluminescence images show representative zircon textures.

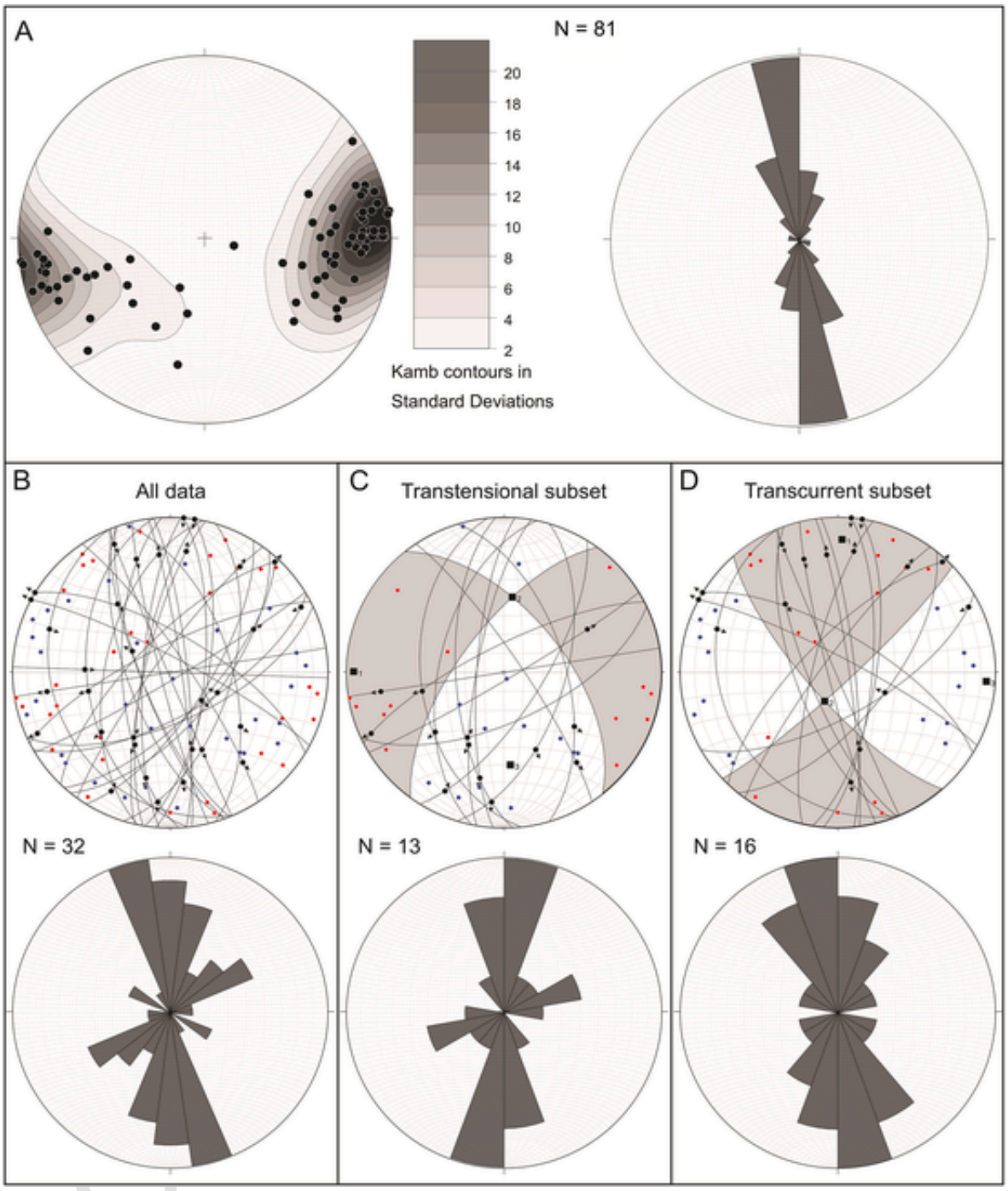

Fig. 7. A. Lower hemisphere, equal-area projection of metamorphic foliation poles. B to D. Kinematic and orientation data of meso-scale faults measured in basement metamorphic rocks. Upper diagrams show kinematic data analyzed with the FaultKinWin® software (Allmendinger et al., 2012). Major circles represent the projection of fault planes in lower hemisphere equal-area projection stereograms, with arrows showing the hanging-wall sense of movement. The distribution of principal incremental shortening (P axes, blue dots) and extension (T axes, red dots) axes is shown for each fault. Black squares represent the obtained axes of the strain ellipsoid (1, 2 and 3) for every group of faults. The number of field data (N) is indicated in each case. Below, lower hemisphere, equal-area projection of fault orientations is shown. B. Complete dataset of faults. C. Faults subset compatible with a transtensional deformation regime. D. Faults subset compatible with a strike-slip deformation regime.

NW-SE left-lateral strike-slip faults characterize this second subset. Only 3 data were discarded, as they were not compatible with the identified subsets.

5. Discussion

5.1. Jurassic magmatism and structural controls

The role of structural inheritance in Jurassic tectono-magmatic processes has been ubiquitously documented in northern Patagonia (Coira et al., 1975; Giacosa and Heredia, 2004b; Renda et al., 2019; Oriolo et al., 2019; Giacosa, 2020; Benedini et al., 2021, 2022). In the particular case of the Jurassic batholith of the North Patagonian Andes in the Bariloche area, Castro et al. (2011) observed similarities between magmatic fabrics of plutons yielding U-Pb SHRIMP ages of ca. 173-150 Ma and those of the metasedimentary wallrock. Furthermore, EPMA Th-U-Pb monazite ages of 171 ± 9 Ma and 170 ± 7 Ma were reported in basement schists and paragneisses, and were interpreted as evidence of retrograde metamorphism under low-pressure conditions and deformation (Oriolo et al., 2019). Comparably, an EPMA Th-U-Pb monazite age of 169 ± 7 Ma was obtained in the Cerro Catedral in a mylonitic mica-schist (Martínez et al., 2023).

Structural, microstructural and geochronological data of the Paso de las Nubes area further confirms the relationship between Jurassic magma emplacement and basement reactivation. The obtained U-Pb LA-ICP-MS zircon age of 166 ± 2 Ma is within the range of Jurassic intrusions of the region constrained by several authors (Castro et al., 2011; Zaffarana et al., 2020; Boltshauser et al., 2023). This orthogneiss was emplaced along the metamorphic foliation of the wallrock (possibly corresponding to the regional S2 reported by previous authors), which shows a significant retrograde overprint (Fig. 5), in line with comparable Jurassic retrograde metamorphism reported in adjacent basement areas constrained by monazite petrochronologic data (see above; Oriolo et al., 2019; Martínez et al., 2023).

Microstructures of fine-grained recrystallized quartz grains suggest bulging recrystallization, and a subordinate role of subgrain rotation, which are further supported by the grain size of recrystallized quartz crystals (Stipp et al., 2002). Therefore, maximum deformation conditions are constrained to ca. 300–350 °C (Stipp et al., 2002), suggesting greenschist facies conditions. On the other hand, relics of granophyric intergrowths, also reported in a Jurassic granite by Castro et al. (2011) and in the La Hoya pluton by Zaffarana et al. (2020), together with spherulites, indicate shallow emplacement conditions of a subvolcanic protolith, in line with low-pressure conditions constrained by barometric data of coeval plutons (Castro et al., 2011; Boltshauser et al., 2023). The development of these igneous textures controlled by deformational microstructures (e.g., granophyric intergrowths in strain shadows) may suggest that solid-state deformation was associated with magma emplacement.

On the other hand, kinematic data record a first population indicating a transtensional setting, which is attributed to Jurassic deformation (Fig. 7). Although with a small sample size (N = 13), this solution shows E-W to ENE-WSW T-axis directions and fault planes striking NNW-SSE (right-lateral) and NNE-SSW (left-lateral). It can be inferred that the basement foliation with comparable orientations might have exerted control on the development of these mesoscale structures associated with this early deformation event. The presence of Jurassic transtension is in line with petrologic data of Jurassic granitoids of the region pointing to a rather thin crust, as revealed by relatively low Sr/Y and La_N/Yb_N contents, and negative Eu anomalies, which indicate plagioclase crystallization in a very shallow crustal level (Castro et al., 2011). Likewise, low P/T conditions were inferred for Jurassic retrograde metamorphism (Oriolo et al., 2019; Martínez et al., 2023).

In sum, the Jurassic subvolcanic-plutonic record of the study area represents one of the deepest exposures of the Jurassic magmatic arc, in contrast to shallower crustal levels recorded to the retroarc region, which are characterized by volcano-sedimentary successions (e.g., Benedini et al., 2022). Dynamics of Jurassic arc magmatism were controlled by slab rollback and oblique subduction, thus accounting for a regional transtensional setting, also well documented in the retroarc region (e.g., Echaurren et al., 2017; Castro et al., 2021; Benedini et al., 2022; Falco et al., 2022).

5.2. Andean Miocene transpression

The western North Patagonian Andes, including the study area, comprise a thick-skinned fold-and-thrust belt with deep structures along the Paleozoic basement, thus highlighting the role of structural inheritance in the Andean orogenic architecture (e.g., Giacosa and Heredia, 2004a, 2004b; Ramos et al., 2014; García et al., 2024). Likewise, basement foliation at Paso de las Nubes strikes NNW-SSE to N-S, with mainly steep dips (Fig. 7A), being thus comparable with the orientation of Miocene faults (Fig. 7; Diraison et al., 1998). This further confirms the role of basement fabric reactivation during Andean Miocene deformation, giving rise to a dextral transpressional regime (Diraison et al., 1998; García et al., 2024).

Neogene dextral transpression is well-documented in the North Patagonian Andes (Diraison et al., 1998; García et al., 2024). Kinematic data obtained herein are similar to those reported by Diraison et al. (1998), being associated with E-W to ENE-WSW shortening (Fig. 7D). When considering regional evidence of thrusting together with computed kinematics of strike-slip-dominated faults, a partitioned transpressional regime can be inferred, as documented in the extra-Andean region as well (García et al., 2024). Comparably, partitioned transpression is well-documented to the west along the Liquiñe-Ofqui Shear Zone, recording coeval Miocene to Pliocene deformation (e.g., Arancibia et al., 1999; De Pascale et al., 2021). Therefore, the dextral orogen-parallel component of displacement resulting from oblique Andean convergence may not only be accommodated by the Liquiñe-Ofqui Shear Zone but also by further structures in the North Patagonian Andes, such as those recorded in the Paso de las Nubes region.

6. Conclusions

As suggested by previous contributions, similarities between metamorphic fabrics of the Paleozoic basement and the magmatic fabrics of the Jurassic plutonic bodies in the study area and surrounding zones, as well as the relative contemporaneity between deformation in the wallrock and their emplacement, are interpreted as an evidence of Jurassic basement reactivation. The U-Pb zircon age of 166 ± 2 Ma obtained in the orthogneiss in Paso de las Nubes is consistent with the development of the Jurassic magmatic arc in the region. Microstructural features document shallow emplacement conditions, controlled by anisotropies of the metamorphic wallrock.

On the other hand, basement fabrics also exerted an important control on fault development during the Jurassic deformational episode. The main NNW-SSE to N-S faults, recording sinistral strike-slip and normal-oblique kinematics, respectively, are concordant with the metamorphic foliation. In addition, fault kinematics indicate that they were developed in a transtensional tectonic regime, with E-W extension and N-S shortening axes. This Jurassic transtensional setting was probably established during slab rollback and oblique subduction, as documented by several authors in northern Patagonia.

Finally, the NNW-SSE to N-S strike-slip faults in the study area are parallel to the basement foliation as well, pointing out again the influence of basement structural inheritance on Neogene deformation. These faults respond to a dextral transpressional regime, which took place during the Miocene Andean deformation phase, also in line with data provided by previous works.

CRediT authorship contribution statement

Sofía Peltzer: Writing – original draft, Visualization, Conceptualization. **María Belén Yoya:** Writing – original draft, Visualization, Conceptualization. **Ezequiel Olaizola:** Writing – review & editing, Data curation. **Florencia Bechis:** Writing – review & editing, Data curation. **Daniel Yagupsky:** Writing – review & editing. **Pablo D. González:** Writing – review & editing. **MiguelA.S. Basei:** Writing – review & editing. **Sebastián Oriolo:** Writing – original draft, Resources, Investigation, Data curation, Conceptualization.

Declaration of competing interest

The authors declare that they have no known competing financial interests or personal relationships that could have appeared to influence the work reported in this paper.

Acknowledgements

We acknowledge the Editors Andrés Folguera and José Allard, and the reviewers Juan Cruz Martínez, Darío Orts and Leonardo Benedini for their comments, suggestions and corrections that were very helpful to improve this work. Sebastián Oriolo thanks financial support of the National Geographic Society (grant CP-123R-17), Agencia Nacional de Promoción Científica y Tecnológica (PICT-2017-1092) and CONICET (PIP 11220200101662CO). Florencia Bechis thanks financial support of the Agencia Nacional de Promoción Científica y Tecnológica (PICT-2014-2240 and PICT-2017-3259).

Data availability

all data are included in the manuscript.

Appendix A. Supplementary data

Supplementary data to this article can be found online at https://doi.org/10.1016/j.jsames.2024.105170.

References

Allmendinger, R.W., 2001. FaultKinWin Version 1.2.2. A Program for Analyzing Fault Slip Data for Windows Computers.

Aragón, E., Castro, A., Díaz-Alvarado, J., Liu, D.Y., 2011. The North Patagonian batholith at Paso Puyehue (Argentina-Chile). SHRIMP ages and compositional features. J. S. Am. Earth Sci. 32, 547–554. https://doi.org/10.1016/j.jsames.2011.02.005.

Arancibia, G., Cembrano, J., Lavenu, A., 1999. Transpresión dextral y partición de la deformación en la Zona de Falla Liquiñe-Ofqui, Aisén, Chile (44-45°S). Rev. Geol. Chile 26, 3–22.

Bechis, F., Cristallini, E.O., 2006. Inflexiones en estructuras del sector norte de la faja plegada y corrida de Nirihuau, Provincia de Río Negro. In: Revista de la Asociación Geológica Argentina, vol. 6. Special Publication, pp. 18–25.

Bechis, F., Encinas, A., Concheyro, A., Litvak, V., Aguirre-Urreta, B., Ramos, V., 2014. New age constraints for the Cenozoic marine transgressions of northwestern Patagonia, Argentina (41°-43° S): paleogeographic and tectonic implications. J. S. Am. Earth Sci. 52, 72–93. https://doi.org/10.1016/j.jsames.2014.02.003.

Benedini, L., Pavón Pivetta, C., Marcos, P., Gregori, D.A., Barros, M., Scivetti, N., Costa dos Santos, A., Strazzere, L., Geraldes, M.C., de Queiróz Bernabé, T., 2021. Lower Jurassic felsic diatreme volcanism recognized in central Patagonia as evidence of along-strike rift segmentation. J. S. Am. Earth Sci. 106, 102705.

Benedini, L., Barros, M., Pavón Pivetta, C., Stremel, A., Gregori, D.A., Marcos, P., Bahía, M., Scivetti, N., Strazzere, L., Geraldes, M., 2022. New insights into the Jurassic polyphase strain partition on the patagonian back-arc; constraints from structural analysis of ancient volcanic structures. Tectonophysics 836, 229–430. https://doi.org/10.1016/j.tecto.2022.229430.

Bilmes, A., D´Elía, L., Franzese, J.R., Veiga, G.D., Hernández, M., 2013. Miocene block uplift and basin formation in the Patagonian foreland: the Gastre Basin, Argentina. Tectonophysics 601, 98–111. https://doi.org/10.1016/j.tecto.2013.05.001.

Butler, R., Tavarnelli, E., Grasso, M., 2006. Structural inheritance in mountain belts: an Alpine-Apennine perspective. J. Struct. Geol. 28, 1893–1908. https://doi.org/10.1016/j.jsg.2006.09.006.

Boltshauser, B.E., Zaffarana, C.B., Gallastegui, G., Orts, D.L., Molina, J.F., Poma, S.M.N., Ruíz González, V., 2023. Petrogenetic evolution and thermobarometry of the Late Jurassic La Hoya pluton, early stages of the North Patagonian batholith, southwestern Argentina. Int. J. Earth Sci. 112, 1687–1716. https://doi.org/10.1007/s00531-023-02320-7.

Butler, K.L., Horton, B.K., Echaurren, A., Folguera, A., Fuentes, F., 2020. Cretaceous-Cenozoic growth of the Patagonian broken foreland basin, Argentina: chronostratigraphic framework and provenance variations during transitions in Andean subduction dynamics. J. S. Am. Earth Sci. 97, 102242. https://doi.org/10.1016/j.jsames.2019.102242.

Castro, A., Moreno-Ventas, I., Fernández, C., Vujovich, G., Gallastegui, G., Heredia, N., Martino, R.D., Becchio, R., Corretge, L.G., Díaz-Alvarado, J., Such, P., García Arias, M., Liu, D., 2011. Petrology and SHRIMP U-Pb zircon geochronology of Cordilleran granitoids of the Bariloche area, Argentina. J. S. Am. Earth Sci. 32, 508–530. https://doi.org/10.1016/j.jsames.2011.03.011.

Castro, A., Rodriguez, C., Fernández, C., Aragón, E., Pereira, M.F., Molina, J.F., 2021. Secular variations of magma source compositions in the North Patagonian batholith from the Jurassic to Tertiary: was mélange melting involved? Geosphere 17, 766–785. https://doi.org/10.1130/GES02338.1.

Cembrano, J., Hervé, F., Lavenu, A., 1996. The Liquiñe Ofqui fault zone: a long-lived intra-arc fault system in southern Chile. Tectonophysics 259, 55–66. https://doi.org/10.1016/0040-1951(95)00066-6.

Clendenin, C.W., Diehl, S.F., 1999. Structural styles of Paleozoic intracratonic fault reactivation: a case study of the Grays Point fault zone in southeastern Missouri, USA. Tectonophysics 305, 235–248. https://doi.org/10.1016/S0040-1951(99)00007-4.

Coira, B.L., Nullo, F., Proserpio, C., Ramos, V.A., 1975. Tectónica de basamento de la región occidental del Macizo Nordpatagónico (prov. de Río Negro y Chubut) República Argentina. Rev. Asoc. Geol. Argent. 3, 361–383.

Davidson, C., Schmid, S.M., Hollister, L., 1994. Role of melt during deformation in the deep crust. Terra. Nova 6, 133–142.

De Pascale, G.P., Froude, M., Penna, I., Hermanns, R.L., Sepúlveda, S.A., Moncada, D., et al., 2021. Liquiñe-Ofqui's fast slipping intra-volcanic arc crustal faulting above the subducted Chile Ridge. Sci. Rep. 11, 7069.

Diraison, M., Cobbold, P.R., Rossello, E.A., Amos, A.J., 1998. Neogene dextral transpression due to oblique convergence across the Andes of northwestern Patagonia, Argentina. J. S. Am. Earth Sci. 11, 519–532. https://doi.org/10.1016/S0895-9811(98)00032-7.

Echaurren, A., Folguera, A., Gianni, G., Orts, D., Tassara, A., Encinas, A., Giménez, M., Valencia, V., 2016. Tectonic evolution of the North Patagonian Andes (41°-44° S) through recognition of syntectonic strata. Tectonophysics 677–678, 99–114. https://doi.org/10.1016/j.tecto.2016.04.009.

Echaurren, A., Oliveros, V., Folguera, A., Ibarra, F., Creixell, C., Lucassen, F., 2017. Early Andean tectonomagmatic stages in north Patagonia: insights from field and geochemical data. J. Geol. Soc. 174, 405–421. https://doi.org/10.1144/jgs2016-087.

Falco, J.I., Hauser, N., Scivetti, N., Reimold, W.U., Schmitt, R.T., Folguera, A., 2022. Upper triassic to middle jurassic magmatic evolution of northern Patagonia: insights from the tectonic and crustal evolution of the los menucos area, North Patagonian Massif, Argentina. J. S. Am. Earth Sci. 113, 103–631. https://doi.org/10.1016/j.jsames.2021.103631.

García-Sansegundo, J., Farias, P., Gallastegui, G., Giacosa, R.E., Heredia, N., 2009. Structure and metamorphism of the gondwanan basement in the Bariloche region (North Patagonian Argentine Andes). Int. J. Earth Sci. 98, 1599–1608. https://doi.org/10.1007/s00531-008-0330-3.

Giacosa, R.E., Heredia, N., 2000. Estructura de los Andes Nordpatagónicos entre los 41° y 42° S, Río Negro y Neuquén, Argentina. IX Congreso Geológico Chileno 571–575.

Giacosa, R.E., Heredia, N., Zubía, M.A., González, R., Faroux, A., Cesari, O., Franchi, M., 2001. Hoja Geológica 4172-IV, San Carlos de Bariloche. Servicio Geológico Minero Argentino.

Giacosa, R.E., Heredia, N., 2004a. Estructura de los Andes Nordpatagónicos en los cordones Piltriquitrón y Serrucho y en el valle de El Bolsón (41° 30´-42° 00´S), Río Negro. Rev. Asoc. Geol. Argent. 59, 91–102.

Giacosa, R.E., Heredia, N., 2004b. Structure of the North Patagonian thick-skinned fold-and-thrust belt, southern central Andes, Argentina (41°-42°S). J. S. Am. Earth Sci. 18, 61–72. https://doi.org/10.1016/j.jsames.2004.08.006.

Giacosa, R., Afonso, J., Heredia, N., Paredes, J.M., 2005. Tertiary tectonics of the sub-andean region of the North Patagonian Andes, southern central Andes of Argentina (41-42°30´S). J. S. Am. Earth Sci. 20, 157–170. https://doi.org/10.1016/j.jsames.2005.05.013.

Giacosa, R.E., 2020. Basement control, sedimentary basin inception and early evolution of the Mesozoic basins in the Patagonian foreland. J. S. Am. Earth Sci. 97, 102407. https://doi.org/10.1016/j.jsames.2019.102407.

Gianni, G., Navarrete, C., Orts, D., Tobal, J., Folguera, A., Giménez, M., 2015. Patagonian broken foreland and related synorogenic rifting: the origin of the Chubut Group Basin. Tectonophysics 649, 81–99. https://doi.org/10.1016/j.tecto.2015.03.006.

Gianni, G.M., Echaurren, A., Folguera, A., Likerman, J., Encinas, A., García, H.P.A., Dal Molin, C., Valencia, V.A., 2017. Cenozoic intraplate tectonics in Central Patagonia: record of main Andean phases in a weak upper plate. Tectonophysics 721, 151–166. https://doi.org/10.1016/j.tecto.2017.10.005.

Gianni, G.M., Dávila, F.M., Echaurren, A., Fennel, L., Tobal, J.E., Navarrete, C., Quezada, P., Folguera, A., Giménez, M., 2018. A geodynamic model linking Cretaceous orogeny, arc migration, foreland dynamic subsidence and marine ingression in southern South America. Earth Sci. Rev. 185, 437–462.

González Díaz, E.F., 1978. Estratigrafía del área de la Cordillera Patagónica entre los paralelos 40°30´y 41° latitud sur (provincia del Neuquén). VII Congreso Geológico Argentino 525–537.

González Díaz, E.F., 1982. Chronological zonation of granitic plutonism in the northern Patagonian Andes of Argentina: the migration of intrusive cycles. Earth Sci. Rev. 18, 365–393. https://doi.org/10.1016/0012-8252(82)90045-9.

Gordon, A., Ort, M.H., 1993. Edad y correlación del plutonismo subcordillerano en las provincias de Río Negro y Chubut (41°-42°30'LS), XII Congreso Geológico Argentino

and II Congreso de Exploración de Hidrocarburos. pp. 120–127.
Gregori, D.A., Rossi, A.C., Benedini, L., 2011. Geocronología de la faja batolítica Aluminé, Provincia de Neuquén, Argentina. XVIII Congreso Geológico Argentino, pp. 93–94.
Haller, M.J., Linares, E., Ostera, H., Page, S., 1999. Petrology and geochronology of the sub-cordilleran plutonic belt of Patagonia. II South American Symposium on Isotope Geology 210–214.
Hervé, F., Moreno, R.H., Parada, M.A., 1974. Granitoids of the andean range of valdivia province, Chile. Pac. Geol. 8, 39–45.
Hervé, M., 1976. Estudio geológico de la Falla Liquiñe-Reloncaví en el área de Liquiñe: antecedentes de un movimiento transcurrente (Provincia de Valdivia). I Congreso Geológico Chileno, pp. 39–56. B.
Hervé, F., Calderón, M., Fanning, M., Pankhurst, R., Rapela, C.W., Quezada, P., 2018. The country rocks of devonian magmatism in the North Patagonian Massif and chaitenia. Andean Geol. 45, 301–317. https://doi.org/10.5027/andgeoV45n3-3117.
Holdsworth, R.E., Butler, C.A., Roberts, A.M., 1997. The recognition of reactivation during continental deformation. J. Geol. Soc. 154, 73–78. https://doi.org/10.1144/gsjgs.154.1.0073.
Holdsworth, R.E., Hand, M., Miller, J.A., Buick, I.S., 2001a. Continental Reactivation and Reworking: an Introduction, vol. 184. Geological Society of London Special Publications, pp. 1–12. https://doi.org/10.1144/GSL.SP.2001.184.
Holdsworth, R.E., Stewart, M., Imber, J., Strachan, R.A., 2001b. The Structure and Rheological Evolution of Reactivated Continental Fault Zones: a Review and Case Study, vol. 184. Geological Society of London Special Publications, pp. 115–137. https://doi.org/10.1144/GSL.SP.2001.184.01.07.
Lavenu, A., Cembrano, J., 1999. Compressional -and transpressional-stress pattern for Pliocene and Quaternary brittle deformation in fore arc and intra-arc zones (Andes of Central and Southern Chile). J. Struct. Geol. 21, 1669–1691. https://doi.org/10.1016/S0191-8141(99)00111-X.
Marrett, R., Allmendinger, R.W., 1990. Kinematic analysis of fault-slip data. J. Struct. Geol. 12, 973–986. https://doi.org/10.1016/0191-8141(90)90093-E.
Martínez, J.C., Dristas, J.A., Massonne, H.-J., 2012. Palaeozoic accretion of the microcontinent Chilenia, North Patagonian Andes: high-pressure metamorphism and subsequent thermal relaxation. Int. Geol. Rev. 54, 472–490. https://doi.org/10.1080/00206814.2011.569411.
Martínez, J.C., Bianchi, F.D., Massonne, H.-J., Dristas, J.A., 2023. Pressure-temperature-deformation evolution of a garnet andalusite-bearing mylonitic micaschist from Cerro Catedral, San Carlos de Bariloche, North Patagonian Andes. XIV Congreso de Mineralogía, Petrología Ígnea y Metamórfica, y Metalogénesis 293–294.
Mella, M., Muñoz, J., Vergara, M., Klohn, E., Farmer, L., Stern, C., 2005. Petrogenesis of the pleistocene tronador volcanic group, andean southern volcanic zone. Andean Geol. 32, 131–154.
Olaizola, E., 2017. Geología y estructura de los alrededores del Paso de las Nubes. Undergraduate thesis, Universidad de Buenos Aires. https://hdl.handle.net/20.500.12110/seminario_nGEO001075_Olaizola.
Oriolo, S., Schulz, B., González, P.D., Bechis, F., Olaizola, E., Krause, J., Renda, E.M., Vizán, H., 2019. The Late Paleozoic tectonometamorphic evolution of Patagonia revisited: insights from the pressure-temperature-deformation-time (P-T-D-t) path of the Gondwanide basement of the North Patagonian Cordillera (Argentina). Tectonics 38, 2378–2400. https://doi.org/10.1029/2018TC005358.
Orts, D.L., Folguera, A., Encinas, A., Ramos, M.E., Tobal, J., Ramos, V.A., 2012. Tectonic development of the North Patagonian Andes and their related Miocene foreland basin (41°30'-43° S). Tectonics 31, 1–24. https://doi.org/10.1029/2011TC003084.
Orts, D.L., Folguera, A., Giménez, M., Ruiz, F., Rojas Vera, E.A., Lince Klinger, F., 2015. Cenozoic building and deformational processes in the North Patagonian Andes. J. Geodyn. 86, 26–41. https://doi.org/10.1016/j.jog.2015.02.002.
Petit, J.P., 1987. Criteria for the sense of movement on fault surfaces in brittle rocks. J. Struct. Geol. 9, 597–608. https://doi.org/10.1016/0191-8141(87)90145-3.
Ramos, M.E., Folguera, A., Fennell, L., Giménez, M., Litvak, V.D., Dzierma, Y., Ramos, V.A., 2014. Tectonic evolution of the North Patagonian Andes from field and gravity data (39-40°S). J. S. Am. Earth Sci. 51, 59–75. https://doi.org/10.1016/j.jsames.2013.12.010.
Ramos, M.E., Tobal, J.E., Sagripanti, L., Folguera, A., Orts, D.L., Giménez, M., Ramos, V.A., 2015. The North Patagonian orogenic front and related foreland evolution during the Miocene, analyzed from synorogenic sedimentation and U/Pb dating (~42°S). J. S. Am. Earth Sci. 64, 467–485. https://doi.org/10.1016/j.jsames.2015.08.006.
Rapela, C.W., Munizaga, F., Dalla Salda, L.H., Hervé, F., Parada, M.A., Cingolani, C., 1987. Nuevas edades K/Ar de los granitoides del sector nororiental de los Andes Patagónicos. X Congreso Geológico Argentino, pp. 18–20.
Rapela, C.W., Pankhurst, R.J., Fanning, C.M., Hervé, F., 2005. Pacific Subduction Coeval with the Karoo Mantle Plume: the Early Jurassic Subcordilleran Belt of Northwestern Patagonia, vol. 246. Geological Society of London, Special Publication, pp. 217–239. https://doi.org/10.1144/GSL.SP.2005.246.01.07.
Renda, E.M., Alvarez, D., Prezzi, C., Oriolo, S., Vizán, H., 2019. Inherited basement structures and their influence in foreland evolution: a case study in Central Patagonia, Argentina. Tectonophysics 772, 228232. https://doi.org/10.1016/j.tecto.2019.228232.
Rosenau, M., Melnick, D., Echtler, H., 2006. Kinematic constraints on intra-arc shear and strain partitioning in the southern Andes between 38°S and 42°S latitude. Tectonics 25 (4). https://doi.org/10.1029/2005TC001943.
Salazar-Mora, C.A., Huismans, R.S., Fossen, H., Egydio-Silva, M., 2018. The wilson cycle and effects of tectonic structural inheritance on rifted passive margin formation. Tectonics 37, 3085–3101. https://doi.org/10.1029/2018TC004962.
Schiffer, C., Doré, A.G., Foulger, G.R., Franke, D., Geoffroy, L., Gernigon, L., Holdsworth, B., Kusznir, N., Lundin, E., McCaffrey, K., Peace, A.L., Petersen, K.D., Phillips, T.B., Stephenson, R., Stoker, M.S., Welford, J.K., 2020. Structural inheritance in the North atlantic. Earth Sci. Rev. 206, 102975. https://doi.org/10.1016/j.earscirev.2019.102975.
Sengor, A.M.C., Lom, N., Sagdic, N.G., 2018. Tectonic inheritance, structure reactivation and lithospheric strength: the relevance of geological history. Geological Society of London Special Publications 470, 105–136. https://doi.org/10.1144/SP470.8.
Stipp, M., Stünitz, H., Heilbronner, R., Schmid, S.M., 2002. The eastern Tonale fault zone: a "natural laboratory" for crystal plastic deformation of quartz over a temperature range from 250 to 750 °C. J. Struct. Geol. 24, 1861–1884. https://doi.org/10.1016/S0191-8141(02)00035-4.
Sutton, J., Watson, J.V., 1986. Architecture of the continental lithosphere. Phil. Trans. Roy. Soc. Lond. 317, 5–12. https://doi.org/10.1098/rsta.1986.0020.
Thatcher, W., 1995. Microplate versus continuum descriptions of active tectonic deformation. J. Geophys. Res. 100, 3885–3894. https://doi.org/10.1029/94JB03064.
Tobal, J.E., Rojas Vera, E., Folguera, A., Ramos, V.A., 2012. Deformación andina en el cordón del Hielo Azul al oeste de El Bolsón. Implicancias en la evolución tectónica de la Cordillera Norpatagónica en Río Negro. Argentina. Andean Geology 39, 442–463.
Tobal, J.E., Folguera, A., Likerman, J., Naipauer, M., Sellés, D., Boedo, F.L., Ramos, V.A., Gimenez, M., 2015. Middle to late Miocene extensional collapse of the North Patagonian Andes (41°30′–42°S). J. S. Am. Earth Sci. 657, 155–171. https://doi.org/10.1016/j.tecto.2015.06.032.
Toubes, R., Spikerman, J., 1973. Algunas edades K/Ar y Rb/Sr de las plutonitas de la Cordillera Patagónica entre los paralelos 40°- 44° de latitud sur. Rev. Asoc. Geol. Argent. 28. 382-39.
Villalba, R., Leiva, J., Rubulls, S., Suarez, J., Lenzano, L., 1990. Climate, tree-ring, and glacial fluctuations in the rio frias valley, rio Negro, Argentina. Arct. Alp. Res. 22, 215–232. https://doi.org/10.1080/00040851.1990.12002786.
White, S.H., Bretan, P.G., Rutter, E.H., 1986. Fault-zone reactivation: kinematics and mechanisms. Phil. Trans. Roy. Soc. Lond. 317, 81–97. https://doi.org/10.1098/rsta.1986.0026.
Yoya, M.B., Oriolo, S., González, P., Restelli, F., Renda, E., Bechis, F., Christie Newbery, J., Marcos, P., Olaizola, E., 2023. The birth of the gondwanide arc: insights into carboniferous magmatism of the North Patagonian Andes (Argentina). J. S. Am. Earth Sci. 123, 104225. https://doi.org/10.1016/j.jsames.2023.104225.
Zaffarana, C.B., Boltshauser, B.E., Ruiz González, V., Orts, D.L., Serra-Varela, S., Puigdomenech, C., 2020. Magmatic and tectonic fabrics in the upper jurassic La Hoya pluton, North Patagonian batholith (~43∘S) as a record of the early stages of the andean deformation. J. S. Am. Earth Sci. 104, 102791. https://doi.org/10.1016/j.jsames.2020.102791.
Zaffarana, C.B., Orts, D.L., Gallastegui, G., Suárez, R., Poma, S., Pernich, S., Aramendía, B., 2024. Reviewing the geochemistry and petrology of the subcordilleran plutonic belt, early jurassic magmatic arc in northern Patagonia. J. S. Am. Earth Sci. 105065.
García, M.R., López, M., Bucher, J., Tettamanti, M., Feo, R., D'Elía, L., Franzese, J.R., 2024. Strain partitioning in the Patagonian Broken Foreland: influence of structural inheritance of early Andean deformation. Journal of the Geological Society 181, 3. https://doi.org/10.1144/jgs2023-166.